



## Determination of binding parameters between lysozyme and its aptamer by frontal analysis continuous microchip electrophoresis (FACMCE)

Marie Girardot<sup>a,b,2</sup>, Hong-Yi Li<sup>a,c,1,2</sup>, Stéphanie Descroix<sup>a,c</sup>, Anne Varenne<sup>a,b,\*</sup>

<sup>a</sup> Laboratory of Physicochemistry of Electrolytes, Colloids and Analytical Sciences, UMR CNRS 7195, France

<sup>b</sup> Ecole Nationale Supérieure de Chimie de Paris (Chimie ParisTech), 11 rue Pierre et Marie Curie, F-75231 Paris cedex 05, France

<sup>c</sup> Ecole Supérieure de Physique et de Chimie Industrielle (ESPCI ParisTech), 10 rue Vauquelin, F-75231 Paris cedex 05, France

### ARTICLE INFO

#### Article history:

Received 4 February 2011

Received in revised form 22 April 2011

Accepted 27 April 2011

Available online 7 May 2011

#### Keywords:

Aptamer

Interaction parameters

Dissociation constant

Number of binding sites

Frontal analysis

Lysozyme

Basic protein

Microchip electrophoresis

### ABSTRACT

An original and simple methodology based on microchip electrophoresis (MCE) in a continuous frontal analysis mode (named frontal analysis continuous microchip electrophoresis, FACMCE) was developed for the simultaneous determination of the binding parameters, *i.e.* ligand–site dissociation constant ( $k_d$ ) and number of binding sites on the substrate ( $n$ ). This simultaneous determination was exemplified with the interaction between an aptamer and its target. The selected target is a strongly basic protein, lysozyme, as its quantification is of great interest due to its antimicrobial and allergenic properties. A glass microdevice equipped with a fluorescence detection system was coated with hydroxypropylcellulose, reducing the electroosmotic flow and adsorption onto the channel walls. This microdevice allowed the continuous electrokinetic injection of a mixture of fluorescently labelled aptamer and non-labelled lysozyme. By determining the concentration of the free fluorescently labelled aptamer thanks to its corresponding plateau height, mathematical linearization methods allowed to determine a  $k_d$  value of  $48.4 \pm 8.0$  nM, consistent with reported results (31 nM), while the average number of binding sites  $n$  on lysozyme, never determined before, was  $0.16 \pm 0.03$ . These results seem to indicate that the buffer nature and the SELEX process should influence the number and affinity of the binding sites. In parallel it has been shown that the binding between lysozyme and its aptamer presents two sites of different binding affinities.

© 2011 Elsevier B.V. All rights reserved.

### 1. Introduction

Aptamers are single-stranded DNA or RNA oligonucleotide sequences which show specific binding affinity towards various targets, ranging from small molecules to proteins, and even whole cells [1–3]. These synthetic molecules are isolated from random-sequence pools by *in vitro* selection thanks to a molecular evolution technique named SELEX (systematic evolution of ligands by exponential enrichment) [4–6]. Aptamers are considered as a nucleic acid version of antibodies, with additional advantages such as low cost, small size, ease of synthesis and labelling, high affinity and increased thermal stability, as well as tolerance to wide range of pH and salt concentration. Aptamers can thus be widely employed

as sensitive diagnosis agents, biomedical research tools and even therapeutics [7–9], and for the development of acoustic or optical biosensors [10–12] and for other separation methods for which aptamers are often used as affinity probes [9,13–17].

To improve the development and use of aptamers in a wide range of domains, it is necessary to develop methods allowing a simple, fast and accurate evaluation of the binding parameters (*i.e.* dissociation constant and stoichiometry) with the target. Methods available for studying biomolecular interactions include spectroscopy, gel filtration chromatography, microdialysis, isothermal calorimetry, surface plasmon resonance and separation techniques such as gel electrophoresis flow induced dispersion analysis (FIDA) [17,21] or capillary electrophoresis (CE) [18–20]. Among the various modes of electrokinetic separations, frontal analysis continuous capillary electrophoresis (FACCE) is an alternative method that involves the continuous electrokinetic injection of the incubated mixture during separation, leading to fronts that are processed as for FACE [31]. FACCE presents the advantage of being simpler in the instrumental process and providing larger fronts for precise height determination.

Since about 15 years, microchip electrophoresis (MCE) has become a powerful alternative to conventional separation methods. Indeed MCE presents further advantages in terms of speed, low sample and reagent consumption, high throughput and inte-

**Abbreviations:** CE, capillary electrophoresis; FACMCE, frontal analysis continuous microchip electrophoresis; MCE, microchip capillary electrophoresis; PB, phosphate buffer.

\* Corresponding author. Tel.: +33 1 44 27 67 11; fax: +33 1 43 26 39 72.

E-mail address: [anne-varenne@chimie-paristech.fr](mailto:anne-varenne@chimie-paristech.fr) (A. Varenne).

<sup>1</sup> Present address: Beijing National Laboratory for Molecular Sciences (BNLMS), Key Laboratory of Bioorganic Chemistry and Molecular Engineering of Ministry of Education; Institute of Analytical Chemistry, College of Chemistry, Peking University, Beijing 100871, China.

<sup>2</sup> Both authors participated equally to this work.

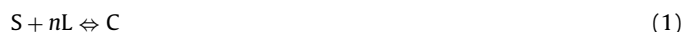
gration capabilities. In this context, different papers have evidenced the interest of MCE for binding characterization. Among them, Gong et al. have used different methods (direct injection or frontal analysis) to study protein–DNA binding [32–34]. In parallel Le Saux et al. exemplified the implementation of continuous frontal analysis in a quartz microchip with UV detection, through measuring inclusion constants of model compounds into  $\beta$ -cyclodextrin by competitive assays [36]. MCE in a continuous frontal analysis mode was also carried out to characterize the binding between a glycopeptide antibiotic teicoplanin (Teic) immobilized on magnetic microspheres, and fluorescently labelled D-Ala–D-Ala terminus peptides [37]. Even if these papers have evidenced the ability of MCE to determine binding constants, most of them used a microdevice with at least a simple-cross or more complicated layout and thus required an optimization of the voltage sequence to drive the sample and electrolyte within the chip. Moreover none of these works allowed to determine the binding stoichiometry of the studied systems; on the contrary, this latter was supposed a priori or from other studies and used to calculate the dissociation constant.

In this work, we report the development of an original and simple methodology based on continuous frontal analysis MCE (that we named frontal analysis continuous microchip electrophoresis, FACMCE) for the determination of the binding parameters, *i.e.* ligand-site dissociation constant ( $k_d$ ) and number of binding sites on the substrate ( $n$ ). The proof of the methodology was demonstrated with lysozyme and its aptamer. Lysozyme is an acid hydrolase which destructs bacterial cells walls, that can be used as biomarker to diagnose or monitor the treatment efficiency of blood diseases such as leukemia [38], or the rejection of organs transplants [39]. Despite its clinical relevance, this system presents some experimental difficulties and has never been completely characterized. Being a strongly basic protein ( $pI=11.35$ ), lysozyme is positively charged under physiological pH and could strongly be adsorbed onto the channel wall due to hydrophobic and electrostatic interactions. The aptamer–lysozyme complex should thus also be adsorbed on the channel walls, causing disruption of the interaction. In addition, under physiological pH, the electrophoretic mobility of the lysozyme-binding aptamer had nearly the same absolute value as the electroosmotic mobility, leading to very long migration times. In order to prevent protein and complex adsorption and to perform rapid separations, a neutral coating was performed on the glass microchip as previously described [43]. The continuous frontal analysis is carried out in a single channel device avoiding any analyte injection step. To deeply investigate the performances of the methodology, the experiments were performed according to two configurations: with (1) varying ligand (*i.e.* aptamer) concentrations and fixed substrate (*i.e.* lysozyme) concentration, and (2) varying substrate concentrations and fixed ligand concentration, the fluorescently labelled ligand being the unique detectable compound. In the first configuration, the determination of the interaction parameters is based on the free ligand concentration, which is directly accessible. Conversely, in the second configuration, the determination of the interaction parameters is based on the free substrate concentration, that is indirectly accessible through the free ligand concentration. The interaction parameters between lysozyme and its aptamer ( $k_d$  and  $n$ ) were determined according to mathematical linearization methods. The results obtained with both configurations were compared to further investigate the aptamer–lysozyme interaction.

## 2. Theoretical [44]

Let us consider an interaction between a substrate (S) and a ligand (L) that can be described by a 1 :  $n$  complex (C). In this case, the

equilibrium can be written (Eq. (1)):



The binding constant ( $K_f = 1/K_d$ ) is then defined as follows (Eq. (2)):

$$K_f = \frac{[C]}{[S][L]^n} \quad (2)$$

where [C], [S] and [L] are the equilibrium concentrations of the complex, free substrate and free ligand, respectively.

In the continuous frontal analysis mode, an incubated substrate/ligand mixture is continuously introduced into the capillary. In most cases, the substrate and the ligand do not play symmetric roles: the partner showing more potential interaction sites (in most cases, the larger one) is usually considered as the substrate, whereas the other partner, supposed to show a unique binding mode, is considered as the ligand. In this case,  $n$  corresponds to the number of binding sites on the substrate. This situation is particularly true for systems of biological interest, such as the interaction between proteins and small molecules. Let us assume that the accessible parameter is the concentration of free ligand, from the height of the plateau following the migration front of the ligand.

If the concentration of the ligand is varied whereas the concentration of the substrate is constant, the binding constant can be obtained from the mass balance equations for the substrate and ligand, yielding the equilibrium complex and free substrate concentrations (Eqs. (3) and (4)):

$$[C] = [S]_0 - [S] = \frac{[L]_0 - [L]}{n} \quad (3)$$

$$[S] = [S]_0 - [C] = [S]_0 - \frac{[L]_0 - [L]}{n} \quad (4)$$

where  $[L]_0$  and  $[S]_0$  are the initial concentrations of the ligand and substrate in the incubated mixture, respectively.

A deeper study employing the multi-site binding model for the determination of the binding parameters expresses the independent binding of one ligand L to one site  $s$  of a given binding strength of a substrate S according to a monomolecular reactional scheme (Eq. (5)):



The binding parameters are in this model the number of binding sites  $n$  belonging to each category and the ligand-site interaction constant  $k_f (=1/k_d)$ , defined as follows (Eq. (6)):

$$k_f = \frac{[s \cdot L]}{[s][L]} \quad (6)$$

The mass balance equation can be expressed as (Eq. (7)):

$$[s]_0 = [s] + [s \cdot L] = n[S]_0 \quad (7)$$

where  $[s]_0$  and  $[s]$  are the initial and free concentrations of the sites.

Data processing can be achieved either by non-linear or linear regressions [45]. In this study, data were treated by performing linearization methods. The binding constant ( $k_f$ ) as well as the number of binding sites ( $n$ ) were simultaneously determined from the equilibrium free ligand concentration [L] according to three mathematical methods for data linearization proposed for the FACCE mode. The mean number of ligands bound to the substrate,  $r$ , is defined as (Eq. (8)):

$$r = \frac{[L]_0 - [L]}{[S]_0} = n \frac{[s \cdot L]}{[s] + [s \cdot L]} = n \frac{k_f[L]}{1 + k_f[L]} \quad (8)$$

and can be directly determined from the free ligand concentration.

Table 1a reports the rearranged equations used in these methods. Even if all equations are equivalent in their algebraic form, the impact of the precision of [L] value depends on whether it appears on numerator or denominator.

**Table 1**  
Binding isotherm and its linearized forms for the determination of binding constants ( $k_f$ ) and stoichiometry ( $n$ ) using the continuous FA mode.

	Method name	Equation	$k_f$ determination	$n$ determination
(a) Variable ligand, constant substrate	Binding isotherm	$r = f([L])$	Slope of the tangent at the origin	Ordinate of the horizontal asymptote
	x-reciprocal (Scatchard plot)	$\frac{r}{[L]} = nk_f - rk_f$	–Slope	–Intercept/slope
	y-reciprocal	$\frac{r}{r} = \frac{1}{nk_f} + \frac{[L]}{n}$	Slope/intercept	1/slope
	Double-reciprocal	$\frac{1}{r} = \frac{1}{nk_f[L]} + \frac{1}{n}$	Intercept/slope	1/intercept
(b) Variable substrate, constant ligand	Binding isotherm	$r_s = f([S])$	Slope of the tangent at the origin	1/Ordinate of the horizontal asymptote
	x-reciprocal (Scatchard plot)	$\frac{r_s}{[S]} = k_f - nk_f r_s$	Intercept	–Slope/intercept
	y-reciprocal	$\frac{r_s}{r_s} = \frac{1}{k_f} + n[S]$	1/intercept	Slope
	Double-reciprocal	$\frac{1}{r_s} = \frac{1}{k_f[S]} + n$	1/Slope	Intercept

If the concentration of the substrate is varied whereas the concentration of the ligand is constant, the mean number of substrate bound to the ligand,  $r_s$ , is defined as (Eq. (9)):

$$r_s = \frac{[S]_0 - [S]}{[L]_0} = \frac{[s - L]}{n([L] + [s - L])} = \frac{k_f[S]}{1 + nk_f[S]} \quad (9)$$

The binding parameters can then be determined from the equilibrium free substrate concentration  $[S]$  using linearization methods very similar to the ones described previously (Table 1b). If the equilibrium free substrate concentration is not directly accessible, it has to be derived from the equilibrium free ligand concentration. As the stoichiometry of the complexation is unknown a priori, it first has to be determined through a direct calculation. A value of  $n$  is arbitrarily chosen, and the binding constant is calculated for each composition of the system thanks to the following equation (Eq. (10)):

$$k_f = \frac{[L]_0 - [L]}{[L] \times (n[S]_0 - [L]_0 + [L])} \quad (10)$$

The value of  $n$  is then optimized in order to minimize the standard deviation on the  $k_f$  values, and  $[S]$  is calculated using Eq. (4). The binding isotherm obtained is linearized according to the three methods, and the dissociation constant  $k_d$  is determined as well as the number of binding sites  $n$ .

### 3. Materials and methods

#### 3.1. Chemicals and reagents

The 30-mer lysozyme-binding aptamer (5'-FAM/ATC AGG GCT AAA GAG TGC AGA GTT ACT TAG-3') was synthesized, labelled with fluorescein phosphoramidite (FAM) at the 5'-end and HPLC-purified by Eurogentec France (Angers, France) and stored at  $-18^\circ\text{C}$  as a 100  $\mu\text{M}$  stock solution in water. Lysozyme from chicken egg white (Mr 14 307, purity 95%), cytochrome c from horse heart (type VI), sodium monobasic phosphate and sodium dibasic phosphate were purchased from Sigma–Aldrich (Saint-Quentin Fallavier, France). Hydroxypropylcellulose (Mr 100,000) was purchased from Scientific Polymer Products (Dean PKWY, Ontario, USA). Standard 1 M NaOH solution Normadoses were provided by VWR (Fontenay-sous-Bois, France).

All samples, solutions and buffers were prepared using analytical-grade chemicals and ultra-pure water produced by a Direct-Q3 system (Millipore, Molsheim, France).

#### 3.2. MCE instrumentation

Monochannel glass microchips were purchased from Micronit Microfluidics (Enschede, The Netherlands). The separation channel was 7.3 cm in length, 20  $\mu\text{m}$  in depth and 50  $\mu\text{m}$  in width. Upchurch reservoirs from Oak (Harbor, USA) were bonded around the wells to increase the reservoir volume. Microchip analysis was monitored by an IX-71 inverted fluorescence microscopic system (Olympus,

France) equipped with a spectral filter 460–490 nm and a 100 W mercury lamp. A CCD camera 1388  $\times$  1038 pixels Pike (RD Vision, France) was mounted on the microscope and Hiris software (RD Vision, France) was used for camera control and image processing. A HVS448 high-voltage power supply (Labsmith, Livermore, USA) was used to apply electric fields to the microchannel through platinum electrodes placed in the reservoirs. All system operations were performed with Labview 7.1 (National Instrument, Austin, USA) programmed through a PC-based computer. All experiments were performed at room temperature.

#### 3.3. Procedures

##### 3.3.1. Microchannel coating procedure

The HPC coating procedure was achieved according to the one previously developed by Poitevin et al. [43]. A 5% (w/v) HPC aqueous solution was prepared. The separation channel was activated by 1 M NaOH and flushed with ultrapure water. Then the channel was filled with the HPC solution from one end of the channel and flushed by air. The two wells were washed with ultra-pure water (Milli-Q) and then liquid in wells was removed. The chip was heated in a GC oven from  $60^\circ\text{C}$  to  $140^\circ\text{C}$  at  $5^\circ\text{C}/\text{min}$ , and maintained at  $140^\circ\text{C}$  for 30 min. After heating, the channel was washed with ultra-pure water. The electroosmotic mobility was estimated according to the procedure developed by Shakalisava et al. [46], which consists in measuring the apparent electrophoretic mobility of 0.01  $\text{mg mL}^{-1}$  fluorescein in a 9 mM sodium borate buffer pH 9.2 knowing its electrophoretic mobility in these conditions ( $-38.0 \times 10^{-5} \text{ cm}^2 \text{ V}^{-1} \text{ s}^{-1}$ ).

##### 3.3.2. FACMCE experiments

Before use, the fluorescently labelled aptamer was activated by heating at  $95^\circ\text{C}$  for 5 min in a water bath and then cooled down to room temperature by itself. After rinsing 3 times with ultrapure water, then with a 30 mM sodium phosphate buffer (PB) (pH 7.5), the separation channel was filled with the separation buffer. One well was filled with the buffer while the other well was filled with the sample, i.e. the aptamer alone or an incubated mixture of aptamer and protein (incubation for 20 min), respectively. The detector was placed in the middle of the channel (effective length, 3.65 cm). A negative voltage of 2200 V (electric field, 300 V/cm) was applied, the cathode being placed in the sample well, so as to achieve a continuous electrokinetic injection of the sample. Meanwhile, fluorescence signal was recorded.

### 4. Results and discussion

Aptamer–protein interactions usually show very small dissociation constants ( $10^{-9}$ – $10^{-11}$  M) [47]. It is thus necessary to analyse the equilibrium at a low concentration range comparable to the dissociation constant in order to determine the binding parameters [22], which requires an adequate detection sensitivity. To our knowledge no microchip format has been used for

aptamer/target full characterization, *i.e.* in terms of ligand-site dissociation constant ( $k_d$ ) and number of binding sites on the substrate ( $n$ ) determination. To investigate the feasibility of such a characterization in a microchip and to perform high throughput characterization while consuming low volume of sample, lysozyme was selected as a target since its quantification shows a great interest in the clinical [38,39] and food industry [40,42] fields. For this aptamer/lysozyme system, a dissociation constant of 31 nM was reported by Ellington *et al.*, by employing standard absorbance assays to measure the inhibition of the lysozyme's cytolytic activity by the aptamer [48].

In this work, a new methodology, FACMCE, coupled with fluorescence detection was developed and therefore used to determine the interaction parameters of the lysozyme–aptamer pair. FACMCE consists in continuously and electrokinetically injecting an incubated mixture of lysozyme and aptamer at different concentrations, leading to fronts. Both the aptamer and the protein could be fluorescently labelled. Nevertheless, in order to avoid multi-labelling [49] and aptamer or protein's charge modification, we decided to perform the labelling on the 5'-end position of the oligonucleotidic sequence, whereas the protein was label free. This labelling position should minimize the probability that it alters the affinity of lysozyme towards the aptamer. The lysozyme being a very basic protein ( $pI > 11$ ), its adsorption onto the channel wall is critical. Preliminary study has shown that a classical hydroxypropylcellulose (HPC) coating avoids the lysozyme adsorption on capillaries (data not shown). A HPC modification of the channel, as developed by Poitevin *et al.* [43], has thus been carried out with glass microchip. The strong reduction of the electroosmotic mobility ( $\mu_{eo} < 3 \times 10^{-5} \text{ cm}^2 \text{ V}^{-1} \text{ s}^{-1}$  in 9 mM sodium borate buffer (pH 9.2)) and the repetability of the migration times (RSD < 3%) obtained by frontal electrophoresis reflected the quality, the stability of the channel modification as well as its ability to avoid protein adsorption.

#### 4.1. Electrophoretic profiles by FACMCE

The limit of detection and the linear range for the labelled aptamer quantitation was studied by electrokinetically and continuously injecting various concentrations of the aptamer (0–1  $\mu\text{M}$ ) in a 30 mM sodium phosphate buffer (PB) (pH 7.5). In these pH conditions, as the aptamer was negatively charged due to the deprotonation of the phosphate groups and the EOF magnitude close to zero, a negative voltage was applied. A front followed by a horizontal plateau was observed at around 30 s, corresponding to an electrophoretic mobility about  $-40 \times 10^{-5} \text{ cm}^2 \text{ V}^{-1} \text{ s}^{-1}$  (Fig. 1) which was consistent with previous results obtained in conventional CZE. This short analysis time should allow high throughput analysis. The limit of detection (LOD) for the aptamer in PB was determined as 10 nM ( $S/N=2$ ) with a linear range of 20–500 nM ( $R^2 = 0.996$ ) (see insert in Fig. 1).

To study the aptamer/lysozyme interaction, a mixture of the labelled aptamer with lysozyme was injected by FACMCE in 30 mM PB (pH 7.5). In these pH conditions, the aptamer was negatively charged, as indicated previously, whereas lysozyme was positively charged due to its high isoelectric point ( $pI = 11.35$ ). Under a negative voltage, the free aptamer migrates into the channel and can be detected as the first front according to the electrophoretic mobility determined at the apex of the front derivative (Fig. 1). No obvious second plateau could be observed even with a 10 min analysis, which means that the aptamer–lysozyme complex was either (i) positively charged and consequently did not migrate into the channel or (ii) negatively charged but with an electrophoretic mobility lower than  $-5 \times 10^{-5} \text{ cm}^2 \text{ V}^{-1} \text{ s}^{-1}$  so that it could not be detected during the 10 min-analysis time, or (iii) not observed due its adsorption on the channel surface (which was however

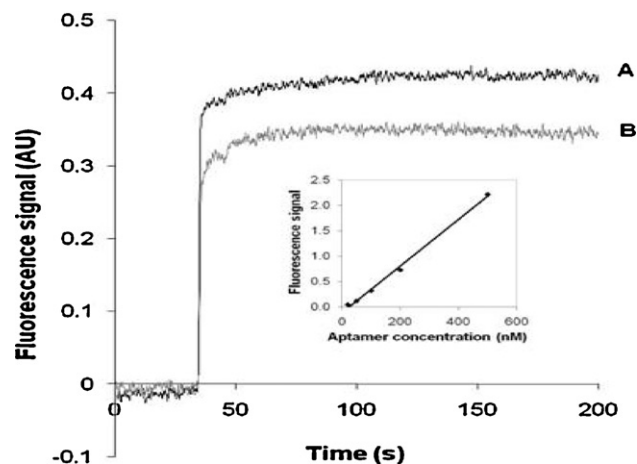


**Fig. 1.** Electropherograms obtained during FACMCE analysis of 80 nM aptamer (A) and 80 nM aptamer mixed with 100 nM lysozyme (B). Insert: calibration curve of the fluorescently labelled aptamer in 30 mM phosphate buffer (pH 7.5) using the optimized experimental conditions. The LOD was 10 nM ( $S/N=2$ ) and the linear range was 20–500 nM. Equation of the least-squares regression straight line ( $n=5$ ):  $y = 0.0046x - 0.1118$ ,  $R^2 = 0.9960$ . Experimental conditions:  $50 \mu\text{m} \times 20 \mu\text{m} \times 7.3 \text{ cm}$  HPC-coated glass microchip (detection length, 3.65 cm). Background electrolyte: 30 mM sodium phosphate (pH 7.5). Applied voltage:  $-2.2 \text{ kV}$ . Temperature:  $25^\circ\text{C}$ . Continuous electrokinetic injection. Sample: lysozyme-binding aptamer at various concentrations.

not experimentally observed). As lysozyme and aptamer are positively and negatively charged, respectively, the net charge of a lysozyme/aptamer complex should be lower whereas the mass increases greatly resulting in a very low electrophoretic mobility of the complex. The aptamer front height allowed the free aptamer concentration determination thanks to the previously established calibration curve (see insert in Fig. 1), and further determination of the binding parameters.

#### 4.2. Interaction parameters determination

So as to study the potential of this methodology, two situations were investigated for the interaction study between lysozyme and its aptamer: (1) incubation of the aptamer in varying concentrations with lysozyme at a fixed concentration and (2) incubation of the aptamer at a fixed concentration with lysozyme in varying concentrations. Given the huge difference in size between the two partners, aptamer was considered as the ligand and lysozyme as the substrate. In the first configuration, the determination of the interaction parameters was based on the free ligand concentration, which was directly accessible. Conversely, in the second configuration, the determination of the interaction parameters was based on the free substrate concentration, so that the lysozyme should be labelled in order to be detected. Yet in order to accurately compare the two configurations, we used the same partners (non-labelled lysozyme and fluorescently labelled aptamer), in the same range of concentration ratios: thus the concentration of free lysozyme had to be indirectly calculated from the concentration of free aptamer.

##### 4.2.1. Incubation of the aptamer in varying concentrations and the lysozyme at a fixed concentration

In this first approach, the aptamer (30–100 nM) was incubated with 100 nM lysozyme. In order to achieve accurate comparison, samples containing the aptamer with or without lysozyme were analyzed in parallel for each aptamer concentration. As expected, the plateau height for free aptamer is obviously decreased in the presence of lysozyme (Fig. 1). When comparing the plateau height of the sample containing the free aptamer without (Fig. 2A) and with lysozyme (Fig. 2B), the interaction parameters were



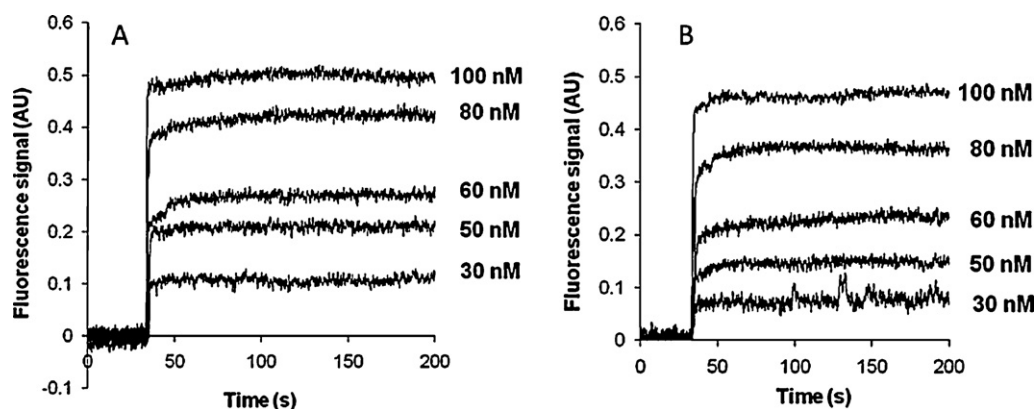


**Fig. 2.** Electropherograms obtained during FACMCE analysis of 30, 50, 60, 80 and 100 nM aptamer alone (A) or mixed with 100 nM lysozyme (B). Experimental conditions: see Fig. 1.

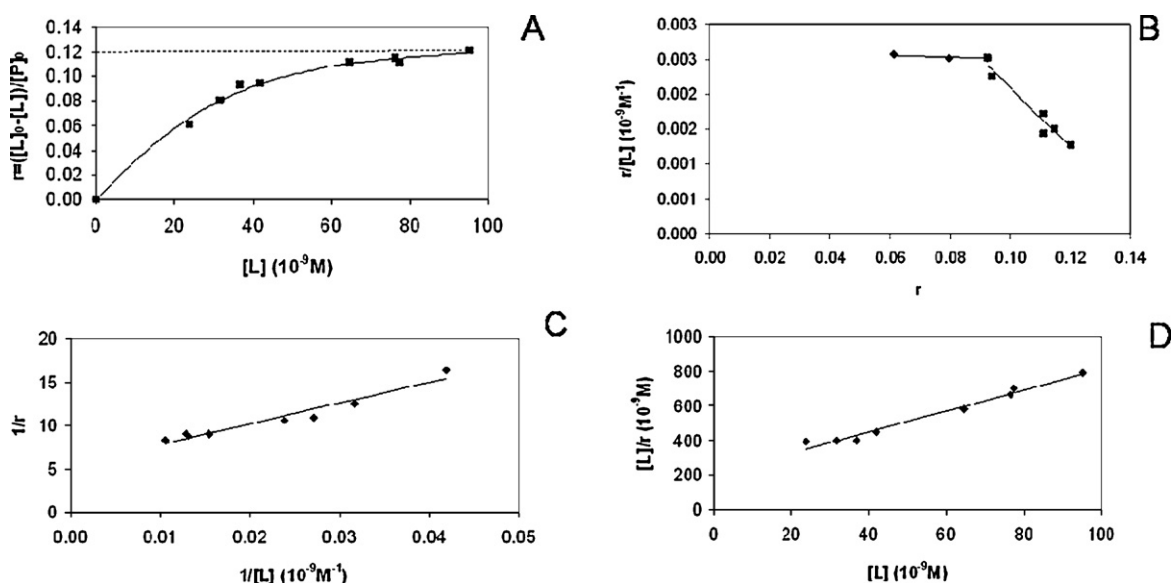


**Fig. 3.** Binding isotherm (A) and its linearization forms according to the  $x$ -reciprocal (B),  $y$ -reciprocal (C) and double-reciprocal (D) methods from experimental data of Fig. 2. Experimental conditions: see Fig. 1, except for the sample which is composed of aptamer in varying concentrations (30–100 nM) mixed with 100 nM lysozyme. Equation of the non-linear regression of the binding isotherm (A):  $y = 6 \times 10^{-8}x^3 - 2 \times 10^{-5}x^2 + 0.0028x$ ,  $R^2 = 0.9969$ . Equations of the least-squares regression straight lines ( $n = 5$ ): (B)  $y = -0.0190x + 0.0034$ ,  $R^2 = 0.8293$ ; (C)  $y = 6.1263x + 273.2000$ ,  $R^2 = 0.9743$ ; (D)  $y = 307.4000x + 5.3766$ ,  $R^2 = 0.9559$ . Segmentation of the  $x$ -reciprocal (Scatchard) plot into two linear parts (B): aptamer concentration range of 30–50 nM (a) of 50–100 nM (b). Equations of the least-squares regression straight lines ( $n = 3$ ): (a)  $y = -0.0039x + 0.0024$  ( $R^2 = 0.4075$ ); (b)  $y = -0.0346x + 0.0049$  ( $R^2 = 0.9977$ ).

determined according to the binding isotherm and three linearization models ( $x$ -reciprocal method,  $y$ -reciprocal method and double-reciprocal method) previously described (Table 1). The experiments reproducibility has been evaluated and RSD inferior to 12% have been achieved for each ratio aptamer/target.

**Table 2**

Binding parameters of the aptamer–lysozyme complex as determined by the FACME method using the binding isotherm and three linearization plotting methods. Sample: (a) aptamer in varying concentrations (30–100 nM) mixed with 100 nM lysozyme or (b) 100 nM aptamer mixed with varying concentrations of lysozyme (100–225 nM).

Method	(a) Variable aptamer		(b) Variable lysozyme	
	$k_d$ (nM)	$n$	$k_d$ (nM)	$n$
Isotherm	34.9	0.12	62.4	0.16
$x$ -rec	54.6	0.18	95.2	0.23
$y$ -rec	45.9	0.17	87.6	0.22
Double-rec	58.0	0.19	74.8	0.22
Average	$49.5 \pm 8.3$	$0.16 \pm 0.03$	$80.0 \pm 14$	$0.21 \pm 0.03$

The results obtained are presented in Fig. 3 and Table 2a, indicating a mean number of binding sites  $n$  on lysozyme of  $0.16 \pm 0.03$  and an average ligand–site dissociation constant ( $k_d$ ) of  $49.5 \text{ nM} \pm 8.3 \text{ nM}$ . This  $k_d$  value corresponds to an average value obtained with the different linearization methods and the standard deviation as well. This latter result is in good accordance with the value of dissociation constant reported by Ellington et al. (31 nM) [48]. As lysozyme and aptamer have opposite charges which could lead to non-specific electrostatic interactions, the specificity of the interaction was checked by replacing lysozyme by cytochrome c that is also a strongly basic protein ( $pK_a \sim 10$ ). No significant variation of the aptamer plateau height was observed when cytochrome c was mixed with aptamer. These results showed the absence of significant non-specific interactions between aptamer and lysozyme in this concentration range and thus validate the obtained  $k_d$  value. Even if low  $n$  values have already been reported in the literature [50,51], no reference value is available for lysozyme and its aptamer. This low  $n$  value obtained could indicate that one aptamer interacts with around 6 proteins. Stampfl et al. have shown that, in the case of neomycin B binding to its aptamer, the aptamer

**Table 3**

Binding parameters of the aptamer–lysozyme complex after segmentation into two binding domains. Sample: (a) aptamer in varying concentrations (30–100 nM) mixed with 100 nM lysozyme or (b) 100 nM aptamer mixed with varying concentrations of lysozyme (100–225 nM).

	Concentration range (nM)	Aptamer/protein ratio ( $x$ )	$k_d$ (nM)	$n$	%
(a) Variable aptamer	30–50	0.3–0.5	$625.4 \pm 50.5$	$1.69 \pm 0.2$	5
	50–100	0.5–1.0	$26.9 \pm 0.2$	$0.15 \pm 0.01$	95
(b) Variable lysozyme	150–225	0.4–0.7	$140.0 \pm 29.4$	$0.28 \pm 0.03$	20
	100–150	0.7–1	$42.4 \pm 0.1$	$0.18 \pm 0.00$	80

underwent a series of up to three consecutive neomycin B binding events, that are associated with distinct conformational changes in the aptamer [50]. At higher neomycin concentration, they have also demonstrated that additional molecules became bound to the aptamer, most probably because of the high positive charges of the amino glycosides, as this facilitated binding to the negative phosphate backbone of the aptamer. Whereas the low molecular mass (Mr 600) of neomycin B could be compatible with a low  $n$  value, in the case of lysozyme (Mr, 14,300) as target, such interactions seem unlikely due to steric hindrance. The  $n$  value estimated could indicate that 16% of the active sites of lysozyme interact with the aptamer. Indeed, the conditions of the SELEX process [48] are quite different compared to the ones used for the affinity measurements. Two critical conditions can especially be mentioned: the lysozyme immobilization on beads via a biotin–streptavidin bond that could induce a specific conformation of the protein [48] and the composition of the SELEX buffer [48,52] (20 mM Tris (pH 7.5), 100 mM NaCl, 5 mM  $MgCl_2$ ).

Interestingly enough, the linearization curve resulting from the  $x$ -reciprocal method, usually referred as “Scatchard plot”, did not present a good linearity ( $R^2 = 0.814$ ), which could indicate a complex interaction. This non-linear behaviour could be obtained when the substrate shows more than one binding domain [44]. The curve was then segmented into two linear parts (Fig. 3B): (i) a linear part corresponding to aptamer concentration in the 30–50 nM range ( $x < 0.5$ , with  $x = [L]_0/[S]_0$  the initial aptamer/protein ratio) with  $R^2 = 0.901$  and (ii) a linear part corresponding to aptamer concentration in the 50–100 nM range ( $0.5 < x < 1$ ) with  $R^2 = 0.923$ . The binding parameters were determined for each part of the curve, and the same process was achieved for the other two linearization forms. The results (Table 3a) suggested the existence, among the population of sites on one protein, of two types of affinity sites, with an average of around 5% for the low affinity sites ( $k_d = 625$  nM,  $n = 1.69$ ) active at low aptamer concentration (30–50 nM,  $x < 0.5$ ), and around 95% for the high affinity sites ( $k_d = 26.9$  nM,  $n = 0.15$ ) active at higher aptamer concentration (50–100 nM,  $0.5 < x < 1$ ).

They are also consistent with the papers of Ruta et al. [53] who have demonstrated the presence of different types of binding sites that are related to different aptamer conformation. Furthermore Stampfl et al. have shown that low neomycin B/aptamer ratios lead to high-affinity binding whereas higher ratios provide lower affinity binding constants [50].

#### 4.2.2. Incubation of the aptamer at a fixed concentration and the lysozyme in varying concentrations

In the reciprocal approach, 100 nM aptamer was incubated with varying lysozyme concentration (100–225 nM). As previously, a negative voltage was applied so that the dissociation constant calculation was based on the plateau height of free aptamer. Since there was no direct access to the free protein concentration, the data were not processed as previously. First,  $n$  was set to 0.15, according to the value determined in the former configuration. Then the dissociation constant ( $k_d$ ) was calculated for each lysozyme concentration using Eq. (10), and  $n$  was optimized so as to provide the lowest standard deviation on the  $k_d$  values. The binding parameters obtained through this optimization allowed the free

protein concentration  $[S]$  to be calculated (Eq. (4)) and the data obtained were linearized (Table 2b). The binding parameters were then derived according to the three methods (results not shown). The value of  $n$  obtained was  $0.21 \pm 0.03$  while the average dissociation constant ( $k_d$ ) was  $80.0$  nM  $\pm 14$  nM (Table 2b). These results were of the same order of magnitude than those obtained in the reversed configuration (Table 2a): the number of binding sites is quite identical, whereas the slight difference in dissociation constant could be explained by the inaccuracy brought by the indirect determination of the concentration of free substrate in this case.

As previously, the Scatchard plot could be segmented into two linear parts with lower  $R^2$  ( $R^2 = 0.689$ ) values than the one of the first configuration. These regions seem to indicate two distinct binding domains on a single protein: (i) around 80% of high affinity sites ( $k_d = 42.4 \pm 0.1$ ,  $n = 0.18 \pm 0.00$ ) in the 100–150 nM lysozyme range ( $0.7 < x < 1$ ) with  $R^2 = 0.83$  and (ii) around 20% of lower affinity sites ( $k_d = 140.0 \pm 29.4$ ,  $n = 0.28 \pm 0.03$ ) in the 150–225 nM lysozyme range ( $0.4 < x < 0.7$ ) with  $R^2 = 0.95$  (Table 3b). These results are quite similar to those obtained previously. The  $x$  ranges are slightly different in the two configurations, this difference could explain the difference obtained in the percentage of low and high affinity sites. However, the first configuration (fixed lysozyme concentration and variable aptamer concentration) seems more convenient and accurate, since the binding parameters are accessible straightforwardly. Thus it will be chosen for the characterization of binding parameters for further studies.

## 5. Concluding remarks

In this work, a new methodology employing frontal analysis in a continuous format in a microsystem (FACMCE) was developed to allow the simultaneous determination of the binding constant and stoichiometry of an interacting system with short analysis time and low sample consumption. It was exemplified with the interaction between a lysozyme-binding aptamer and its target. In order to overcome the difficulties raised by the strong basicity of the protein, the separation channel was permanently coated with a neutral polymer, hydroxypropylcellulose (HPC), which also allowed to strongly reduce the electroosmotic mobility. After optimization of the running conditions, the binding parameters were derived from the free labelled-aptamer plateau height, using mathematical linearization methods. The results obtained showed that the binding between lysozyme and its aptamer presents two sites of different binding affinities. A low aptamer/protein ratio favoured weak sites, whereas a higher aptamer/protein ratio induced a stronger, more specific affinity. The  $n$  values obtained in this study could furthermore indicate the importance of the buffer composition and the SELEX process on the aptamer conformation. The two configurations tested (variable aptamer/ fixed lysozyme and variable lysozyme/ fixed aptamer) led to similar results, although the data processing was slightly different. The configuration where aptamer (*i.e.* the compound which is directly detected) is varied and lysozyme is constant allowed an easier and more direct access to the binding parameters, and could thus be chosen for further experiments. Thus the capability of FACME for characterizing any type of aptamer–protein interactions was demonstrated. This method

is currently used to further investigate the influence of various parameters on the aptamer–target interaction.

## References

- [1] M. Famulok, G. Mayer, M. Blind, *Acc. Chem. Res.* 33 (2000) 591.
- [2] S.D. Jayasena, *Clin. Chem.* 45 (1999) 1628.
- [3] T. Mairal, V.C. Özalp, P.L. Sánchez, M. Mir, I. Katakis, C.K. O'Sullivan, *Anal. Bioanal. Chem.* 390 (2008) 989.
- [4] R. Stoltenburg, C. Reinemann, B. Strehlitz, *Biomol. Eng.* 24 (2007) 381.
- [5] F. Le Floch, H.A. Ho, M. Leclerc, *Anal. Chem.* 78 (2006) 4727.
- [6] T. Sampson, *World Patent Information* 25 (2003) 123.
- [7] R.K. Mosing, M.T. Bowser, *J. Sep. Sci.* 30 (2007) 1420.
- [8] M. Famulok, J.S. Hartig, G. Mayer, *Chem. Rev.* 107 (2007) 3715.
- [9] C. Ravelet, C. Grosset, E. Peyrin, *J. Chromatogr. A* 1117 (2006) 1.
- [10] M. Minunni, S. Tombelli, S. Gulotto, A. Luzi, M. Mascini, *Biosens. Bioelectron.* 20 (2004) 1149.
- [11] M. Liss, B. Petersen, H. Wolf, E. Prohaska, *Anal. Chem.* 74 (2002) 4488.
- [12] R. Kirby, E. Cho, B. Gehrke, T. Bayer, Y.S. Park, D.P. Neikirk, J.T. McDevitt, A.D. Ellington, *Anal. Chem.* 76 (2004) 4066.
- [13] M. Michaud, E. Jourdan, A. Villet, A. Ravel, C. Grosset, E. Peyrin, *J. Am. Chem. Soc.* 125 (2003) 8672.
- [14] S.L. Clark, V.T. Remcho, *Anal. Chem.* 75 (2003) 5692.
- [15] S.L. Clark, V.T. Remcho, *Electrophoresis* 23 (2002) 1335.
- [16] A. Sasolas, L.J. Blum, B.D. Leca-Bouvier, *Analyst* 136 (2011) 257–274.
- [17] Z. Zhu, C. Ravelet, S. Perrier, V. Guieu, B. Roy, C. Perigaud, E. Peyrin, *Anal. Chem.* 82 (2010) 4613.
- [18] J. Østergaard, N.H.H. Heegaard, *Electrophoresis* 24 (2003) 2903.
- [19] M. Jing, M.T. Bowser, *Anal. Chim. Acta* 686 (2011) 9.
- [20] J. Oravcová, B. Böhs, W.J. Lindner, *J. Chromatogr. B* 677 (1996) 1.
- [21] H. Jensen, J. Oestergaard, *J. Am. Chem. Soc.* 132 (2010) 4070.
- [22] K. Shimura, K.I. Kasai, *Anal. Biochem.* 251 (1997) 1.
- [31] J.Y. Gao, P.L. Dubin, B.B. Muhoberac, *Anal. Chem.* 69 (1997) 2945.
- [32] M. Berezovski, R. Nutiu, Y. Li, S.N. Krylov, *Anal. Chem.* 75 (2003) 1382.
- [33] I. German, D.D. Buchanan, R.T. Kennedy, *Anal. Chem.* 70 (1998) 4540.
- [34] M. Gong, K.R. Wehmeyer, P.A. Limbach, W.R. Heineman, *Electrophoresis* 28 (2007) 837.
- [36] T. Le Saux, H. Hisamoto, S. Terabe, *J. Chromatogr. A* 1104 (2006) 352.
- [37] X. Liu, F.A. Gomez, *Anal. Bioanal. Chem.* 393 (2009) 615.
- [38] C. Sexton, D. Buss, B. Powell, M. O'Connor, R. Rainer, R. Woodruff, J. Cruz, M. Pettenati, P.N. Rao, L.D. Case, *Leukemia Res.* 20 (1996) 467.
- [39] J.W. Jones, S. Su, M.B. Jones, B.T. Heniford, K. McIntyre, D.K. Granger, *J. Surg. Res.* 84 (1998) 134.
- [40] V.A. Proctor, F.E. Cunningham, *Food Sci. Nutr.* 26 (1988) 4.
- [42] R. Marchal, D. Chaboche, L. Marchal-Delahaut, C. Gerland, J.P. Gandon, P. Jean-det, *J. Agric. Food Chem.* 48 (2000) 3225.
- [43] M. Poitevin, Y. Shakalisava, S. Miserere, G. Peltre, J.L. Viovy, S. Descroix, *Electrophoresis* 30 (2009) 4256.
- [44] K.A. Connors, *Binding Constants. The Measurements of Molecular Complex Stability*, John Wiley & Sons, New York, 1987.
- [45] M.T. Bowser, D.D.Y. Chen, *J. Phys. Chem. A* 103 (1999) 197.
- [46] Y. Shakalisava, M. Poitevin, J.L. Viovy, S. Descroix, *J. Chromatogr. A* 1216 (2009) 1030.
- [47] L. Gold, B. Polisky, O. Uhlenbeck, M. Yarus, *Ann. Rev. Biochem.* 64 (1995) 763.
- [48] J.C. Cox, A.D. Ellington, *Bioorg. Med. Chem.* 9 (2001) 2525.
- [49] I. Le Potier, G. Franck, C. Smadja, S. Varlet, M. Taverna, *J. Chromatogr. A* 1046 (2004) 271.
- [50] S. Stampfl, A. Lempradl, G. Koehler, R. Schroeder, *ChemBioChem* 8 (2007) 1137.
- [51] C. Andre, A. Xicluna, Y.C. Guillaume, *Electrophoresis* 26 (2005) 3247.
- [52] M. Girardot, P. Gareil, A. Varenne, *Electrophoresis* 31 (2010) 546.
- [53] J. Ruta, C. Ravelet, C. Grosset, J. Fize, A. Ravel, A. Villet, E. Peyrin, *Anal. Chem.* 78 (2006) 3032.